OUTP-0114P
15 March 2001

Scalar Glueball-$q\bar{q}$ Mixing above 1 GeV and implications for Lattice QCD

Frank E. Close[1]

Dept of Theoretical Physics
University of Oxford
1 Keble Rd, Oxford, OX1 3NP,UK

Andrew Kirk[2]

School of Physics and Astronomy
Birmingham University, Birmingham, B15 2TT

Abstract

Lattice QCD predictions have motivated several recent studies of the mixing between the predicted $J^{PC} = 0^{++}$ glueball and a $q\bar{q}$ nonet in the $1.3 \rightarrow 1.7$ GeV region. We show that results from apparently different approaches have some common features, explain why this is so and abstract general conclusions. We place particular emphasis on the flavour dependent constraints imposed by decays of the $f_0(1370)$, $f_0(1500)$ and $f_0(1700)$ to all pairs of pseudoscalar mesons. From these results we identify a systematic correlation between glueball mass, mixing, and flavour symmetry breaking and conclude that the glueball may be rather lighter than some quenched lattice QCD computations have suggested. We identify experimental tests that can determine the dynamics of a glueball in this mass region and discuss quantitatively the feasibility of decoding glueball-$q\bar{q}$ mixing.

[1]e-mail: F.E.Close@rl.ac.uk
[2]e-mail: ak@hep.ph.bham.ac.uk

1 Introduction

The best estimate for the masses of glueballs comes from lattice gauge theory calculations, which in the quenched approximation show [1] that the lightest glueball has $J^{PC} = 0^{++}$ and that its mass should be in the range $1.45 - 1.75$ GeV. While the lattice remains immature for predicting glueball decays, Amsler and Close [2, 3] first pointed out that in lattice inspired models, such as the flux tube [4], glueballs will mix strongly with nearby $q\bar{q}$ states with the same J^{PC} [5]. Recent studies on coarse-grained lattices appear to confirm that there is indeed significant mixing between G and $q\bar{q}$ together with associated mass shifts, at least in the $J^{PC} = 0^{++}$ sector [6]. If these results survive at finer lattice spacing, the conclusion will be that glueball-flavour mixing is a controlling feature of the phenomena in the $\sim 1.3 - 1.7$ GeV mass region of meson spectroscopy. It is our purpose in the present paper to build a phenomenological interpretation of the data based on intuition from lattice QCD, and to identify the data needed to confirm it.

To help orient readers, we first present an overview of the paper and its central conclusions.

The first analyses of $G - q\bar{q}$ mixing used the mass matrix with an assumed $G - q\bar{q}$ mixing strength [2, 3, 7, 8, 9, 10]. Such a mixing between a glueball and a $q\bar{q}$ nonet will lead to three isoscalar states of the same J^{PC}. Motivated by Lattice QCD, these analyses focussed on the physical states in the glueball mass region - the $f_0(1370)$ and $f_0(1500)$ and either predicted the existence of a further $J = 0$ state around 1700 MeV [2, 3] or assumed that the $f_J(1710)$ was that state [8]. The existence of this scalar meson is now experimentally verified [11].

These papers differed in what they assumed for the mass of the bare glueball relative to the $S \equiv s\bar{s}$, which led to some quantitative differences in output. Nonetheless, while these papers at first sight differed in detail, their conclusions share some common robust features. In particular, the flavour content of the states is predicted to have the $n\bar{n}$ and $s\bar{s}$ in phase (SU(3) singlet tendency) for the $f_0(1370)$ and $f_0(1710)$, and out of phase (octet tendency) for the $f_0(1500)$. In section 2 we review these papers and show why their outputs are similar. In particular these similarities highlight that further constraints are needed if we are to establish whether the bare glueball is at the upper [8, 10] or lower [2, 3] end of the $1.45 - 1.75$ GeV range favoured by quenched lattice QCD, or even whether the glueball is required [12].

There are now extensive data on the production and decay [13] of the above states. These provide further constraints on the $G - q\bar{q}$ content. Theoretical analysis of decays is under better control than production and so we shall discuss the implications of decays first (section 3).

The WA102 collaboration has published [14], for the first time in a single experiment, a complete data set for the decay branching ratios of the $f_0(1370)$, $f_0(1500)$ and $f_0(1710)$ to all pseudoscalar meson pairs. Ref. [9] and a preliminary letter by us [15] have examined the flavour dependence of scalar meson decay and how these data constrain the flavour and glue mixing of these scalar states. The results here too agree with the generic structure found in the mass mixing analyses of section 2. We identify why this is so and assess the implications. A result that is more general than any specific mixing scheme is that no pair out of the three $f_0(1370)$, $f_0(1500)$, $f_0(1710)$ can be in the same pure $q\bar{q}$ nonet; other degrees of freedom are required.

We shall see that the results are robust. They confirm lattice results that $G - q\bar{q}$ mixing is (nearly) flavour blind and suggest that the preferred glueball mass falls into the mass range, $\frac{M_S+M_N}{2} > M_G \geq M_N$. Then (section 3.2) we will investigate the stability against flavour symmetry breaking. From these results we shall identify a systematic correlation between glueball mass, mixing, and flavour symmetry breaking. To choose among these results requires further experimental tests that can determine the dynamics of a glueball in this mass region. This brings us to section 5 and production dynamics.

Production by $\gamma\gamma$ is potentially the cleanest as this probes the

$q\bar{q}$ flavours and phases. We advocate serious study of $\gamma\gamma \to 0^{++}$ as the sharpest arbiter of the wavefunctions, but we also warn against overly naive interpretation of $\gamma\gamma$ couplings in the 0^{++} sector. The angular and kinematic dependence of $pp \to pp + 0^{++}$ also shows distinct differences among the various mesons, but the dynamical origin of this is still obscure. We note a possible systematic pattern that correlates the G and flavour mixing in our solutions with the distributions observed in central production. Further ways of separating the $G - q\bar{q}$ content in the 0^{++} sector are proposed. Ideally $\gamma\gamma$ couplings can disentangle the amplitudes and this can then be used to decode the dynamics of central production.

2 Mass Mixing

Based upon intuition from lattice QCD, refs. [2, 8, 16] investigated the mixing between a $J^{PC} = 0^{++}$ glueball, G, and a $J^{PC} = 0^{++}$ $q\bar{q}$ nonet in its vicinity. The detailed assumptions of the two approaches differed but the outputs were remarkably similar in certain features. We shall first illustrate why this similarity occurs, abstract its general features and then propose further tests of the general hypothesis.

In the $|G\rangle \equiv |gg\rangle$, $|S\rangle \equiv |s\bar{s}\rangle$, $|N\rangle \equiv |u\bar{u} + d\bar{d}\rangle/\sqrt{2}$ basis, the mass matrix describing the $G - q\bar{q}$ mixing was written as follows in ref. [8]:

$$M = \begin{pmatrix} M_G & f & \sqrt{2}fr \\ f & M_S & 0 \\ \sqrt{2}fr & 0 & M_N \end{pmatrix}. \tag{1}$$

Here $f \equiv \langle G|M|S\rangle$ and $r \equiv \langle G|M|N\rangle/\sqrt{2}\langle G|M|S\rangle$ are the mixing strengths between the glueball and the quarkonia states. For a $G - q\bar{q}$ coupling that is flavour blind, $r = 1$. Lattice QCD [8] finds for $J^{PC} = 0^{++}$ that $r = 1.20 \pm 0.07$. M_G, M_S and M_N represent the masses of the bare states $|G\rangle$, $|S\rangle$ and $|N\rangle$, respectively.

Refs. [2, 8] assumed that the mixing is strongest between the glueball and nearest $q\bar{q}$ neighbours. With the lattice (in the quenched approximation) predicting the glueball mass to be in the $1.45 - 1.75$ GeV region, this has naturally led attention to focus on the physical states $|f_0(1710)\rangle$, $|f_0(1500)\rangle$ and $|f_0(1370)\rangle$ as the eigenstates of M with the eigenvalues of M_1, M_2 and M_3, respectively. The three physical states can be read as [9, 15]

$$\begin{pmatrix} |f_0(1710)\rangle \\ |f_0(1500)\rangle \\ |f_0(1370)\rangle \end{pmatrix} = U \begin{pmatrix} |G\rangle \\ |S\rangle \\ |N\rangle \end{pmatrix} = \begin{pmatrix} x_1 & y_1 & z_1 \\ x_2 & y_2 & z_2 \\ x_3 & y_3 & z_3 \end{pmatrix} \begin{pmatrix} |G\rangle \\ |S\rangle \\ |N\rangle \end{pmatrix}, \tag{2}$$

where

$$U = \begin{pmatrix} (M_1-M_S)(M_1-M_N)C_1 & (M_1-M_N)fC_1 & \sqrt{2}(M_1-M_S)rfC_1 \\ (M_2-M_S)(M_2-M_N)C_2 & (M_2-M_N)fC_2 & \sqrt{2}(M_2-M_S)rfC_2 \\ (M_3-M_S)(M_3-M_N)C_3 & (M_3-M_N)fC_3 & \sqrt{2}(M_3-M_S)rfC_3 \end{pmatrix} \tag{3}$$

with $C_{i(i=1,\ 2,\ 3)} = [(M_i - M_S)^2(M_i - M_N)^2 + (M_i - M_N)^2 f^2 + 2(M_i - M_S)^2 r^2 f^2]^{-\frac{1}{2}}$ and $\Sigma M_{1+2+3} \equiv \Sigma M_{G+S+N}$.

To focus discussion, we first summarise and compare various mixings that have been proposed in the literature. In the original analysis of the glueball-$q\bar{q}$ mixing, ref. [2, 3] worked at leading order in perturbation and obtained

$$\begin{aligned} N_G|\Psi_1\rangle &= |G\rangle + \xi(\sqrt{2}r|N\rangle + \omega|S\rangle) \\ N_s|\Psi_2\rangle &= |S\rangle - \xi\omega|G\rangle \\ N_n|\Psi_3\rangle &= |N\rangle - \xi\sqrt{2}r|G\rangle \end{aligned} \tag{4}$$

where the N_i are appropriate normalisation factors, $\omega \equiv \frac{M_G - M_N}{M_G - M_S}$ and the mixing parameter $\xi \equiv \frac{f}{M_G - M_N}$. This leading form is strictly only valid when both ξ and $\xi\omega << 1$. The 3×3 matrix, eqs. (1)-(3) effectively generalised this to $O(\xi^2)$. The pQCD analysis of ref. [7] suggested that the $gg \to q\bar{q}$ mixing amplitude manifested in $\psi \to \gamma R(q\bar{q})$ is qualitatively $\sim O(\alpha_s) \sim 0.5$. While the absolute value of ξ was not precisely determined, it nonetheless suggested that $O(\xi^2)$ effects may be significant, as in eqs. (2,3). In particular this introduces N into Ψ_2 and S into Ψ_3.

Mixing based on lattice glueball masses leads to two classes of solution of immediate interest:

(i) $\omega \leq 0$, corresponding to G in the midst of the nonet [2]

(ii) $\omega > 1$, corresponding to G above the $q\bar{q}$ members of the nonet [8].

The model of Genovese [10] is a particular case where the G and S are degenerate; mathematically his solution is subsumed in eq. (4) when $\xi \to 0$; $\omega \to \infty$ with $\xi\omega \to 1$.

Weingarten [8] constructed his mixing model based on the scenario from lattice QCD that the scalar $s\bar{s}$ state, in the quenched approximation, may lie lower than the scalar glueball [8, 17] (thus $\omega > 1$ in the above formalism). In their most recent computation of ref. [8], the input "bare" masses were $M_N = 1470$ MeV; $M_S = 1514$ MeV; $M_G = 1622$ MeV and the mixing strength $f \equiv \xi \times (M_G - M_N) = 64 \pm 13$ MeV, whereby $\xi \sim 0.4 \pm 0.1$. The resulting mixtures, with errors shown in parentheses, are (up to an overall phase)

$$\begin{array}{cccc} & f_{i1}^{(G)} & f_{i2}^{(S)} & f_{i3}^{(N)} \\ f_0(1710) & 0.86(5) & 0.30(5) & 0.41(9) \\ f_0(1500) & -0.13(5) & 0.91(4) & -0.40(11) \\ f_0(1370) & -0.50(12) & 0.29(9) & 0.82(9) \end{array} \tag{5}$$

It is instructive to compare this with the assumption of ref. [2, 3] where, for example,the G lies between $n\bar{n}$ and $s\bar{s}$ such that the parameter $\omega \sim -2$. At first sight this would appear to be quite different to the above, but if for illustration we adopt $\xi = 0.5 \sim \alpha_s$, the resulting mixing amplitudes are

$$\begin{array}{cccc} & f_{i1}^{(G)} & f_{i2}^{(S)} & f_{i3}^{(N)} \\ f_0(1710) & 0.60 & 0.76 & 0.22 \\ f_0(1500) & -0.61 & 0.61 & -0.43 \\ f_0(1370) & -0.50 & 0.13 & 0.86 \end{array} \tag{6}$$

It is immediately apparent that the solutions for the lowest mass state in the two schemes are similar, as are the relative phases throughout and also the qualitative importance of the G component in the high mass state. Both solutions exhibit destructive interference between the N and S flavours for the middle state.

This parallelism is not a coincidence. The essential dynamical assumption of ref. [8] and here is that the basic $G - q\bar{q}$ coupling is (nearly) flavour symmetric. A general feature of such a three way mixing is that in the extreme limit of infinitely strong mixing the central state would tend towards flavour octet with the outer (heaviest and lightest) states being orthogonal mixtures of glueball and flavour singlet, namely

$$\begin{array}{ccc} f_0(1710) & \rightarrow & |q\bar{q}(\mathbf{1})\rangle + |\mathbf{G}\rangle \\ f_0(1500) & \rightarrow & |q\bar{q}(\mathbf{8})\rangle + \epsilon|\mathbf{G}\rangle \\ f_0(1370) & \rightarrow & |q\bar{q}(\mathbf{1})\rangle - |\mathbf{G}\rangle \end{array} \tag{7}$$

where $\epsilon \sim \xi^{-1} \rightarrow 0$. In effect, in such an extreme case the glueball would have leaked away maximally to the outer states even in the case (ref. [2, 3]) where the bare glueball (zero mixing) was in the middle of the nonet to start with. The leakage into the outer states becomes significant once the mixing strength (off diagonal term in the mass matrix) becomes comparable to the mass gap between glueball and $q\bar{q}$ states (i.e. either $\xi \geq 1$ or $\xi\omega \geq 1$). Even in the zero width approximation of ref. [2, 3] this tends to be the case and when one allows for the widths being of $O(100)$ MeV while the nonet masses and glueball mass are themselves spread over only a few hundred MeV, it is apparent that there will be considerable mixing of the glueball into the $q\bar{q}$ nonet. The tendency for the $q\bar{q}$ content to separate into two constructive ("singlet tendency") and one destructive ("octet tendency") happens for even mild mixing; the complete leakage of glueball from the latter is only effected as the mixing indeed tends towards infinity.

If the $G - q\bar{q}$ coupling is flavour dependent, such that (as above)

$$r \equiv \langle G|M|N\rangle/\sqrt{2}\langle G|M|S\rangle \neq 1 \tag{8}$$

the "asymptotic maximal mixing" solution will reflect this. Specifically (up to overall normalisation factors)

$$\begin{array}{ccc} f_0(1710) & \rightarrow & |G\rangle + \frac{1}{\sqrt{2r^2+1}}|\sqrt{2}rN + S\rangle \\ f_0(1500) & \rightarrow & \epsilon|G\rangle + \frac{1}{\sqrt{2r^2+1}}|N - \sqrt{2}rS\rangle \\ f_0(1370) & \rightarrow & -|G\rangle + \frac{1}{\sqrt{2r^2+1}}|\sqrt{2}rN + S\rangle \end{array} \tag{9}$$

The pattern of N and S phases in equations (5) and (6), namely two constructive and one destructive, emerge so long as $r > 0$. The lattice results of ref. [8] imply $r = 1.20 \pm 0.07$. It is for these reasons, *inter alia*, that the output of refs. [2, 3, 7, 8] and [9, 15] are rather similar. In contrast, ref. [18] finds opposite phases to the above and this is because their mass matrix has $r < 0$, which would correspond to the mixing being driven by octet. This differs radically from what would be expected for mixing driven by a glueball. In the flavour symmetry limit, a glueball transforms as a flavour singlet; there is a small octet component, if the above results of lattice QCD [8] are a guide, but the idea that it should be orthogonal to this and dominantly octet seems bizarre. We note the mathematical consistency whereby if $r \to -r$ in ref. [18], their conclusions and results would parallel those reported here, but for the reasons just outlined, this is so far from the lattice expectation that we do not discuss it further.

The sharing of the glueball intensity among the three states is driven by the proximity of the glueball to the bare states, amplified by their $n\bar{n}$ contents (due to the factor $\sqrt{2}$ relative amplitude for coupling to $n\bar{n}$ versus $s\bar{s}$). Apart from this, the overall qualitative pattern of phases makes it hard to distinguish among them. So the debate about whether the bare glueball lies within [2, 3] or above [8] a prominent $q\bar{q}$ nonet may be academic unless fine measurement of the quantitative rather than simply qualitative pattern can be extracted from data. However, this robust general feature of the phase pattern enables this picture of glueball-nonet mixing to be disproved if their common implications fail empirically.

In this context we draw attention to the non-trivial implications of these dynamics for the flavour content of the $f_0(1500)$. While there has been considerable debate about the nature of this state, there is rather general agreement empirically that the flavour content of the $f_0(1500)$ has N and S out of phase. It is interesting that this emerges naturally, and as a necessary consequence, for the "middle" member when $G - q\bar{q}$ mixing is involved. While not a proof, this adds weight to the hypothesis that the $f_0(1500)$ is in a trio, with one partner higher and one lower in mass.

Conversely, had the $f_0(1500)$ not had these characteristics then this dynamics could have been eliminated.

Since those mass mixings were first discussed, there have emerged extensive data on the flavour-dependence of these states' decays into pairs of pseudoscalar mesons. Analysis of these decays can be used to give measures of the flavour composition of these scalars, which bear no a priori relation to the mass mixing arguments. As such they provide an independent check on the above. We shall now examine this in section 3.

3 Mixing and Decays

The WA102 Collaboration at CERN has published a complete set of decay branching ratios for the $f_0(1370), f_0(1500)$ and $f_0(1710)$ to all kinematically allowed combinations of pairs of pseudoscalars [14]. These relative strengths depend upon the flavour content of the scalars. The challenge is to decode this information and to compare the resulting pattern with that deduced from the mass mixings above.

We shall use the WA102 data in our primary analysis. If instead we use a world average, our conclusions are stable (shown in section 3.1.1). In order to reduce model dependence, we shall take intuition from the flux tube model [19], which is based on lattice QCD. This suggests three major pathways for triggering the decays [3],

(i) the direct coupling of the quarkonia component of the three states to the final pseudoscalar mesons (PP) (fig. 1a),

(ii) the decay of $gg \to q\bar{q}q\bar{q}$ as in fig. 1b. The resulting amplitudes can be obtained from eqs. (A4) of ref. [2] and have overall strength r_2 (to be fitted) relative to the mode (i) [9, 15].

Finally, following ref. [2, 20], we allow for (iii) in fig. 1c, the direct coupling of the glue in the initial state to isoscalar mesons (i.e. $\eta\eta$ and $\eta\eta'$ decays) and allow r_3 to be the ratio of mode (iii) to (i) [9, 15].

In order to unfold the production kinematics we use the invariant decay couplings (γ_{ij}) for the observed decays, namely we express the partial width (Γ_{ij}) as [2]

$$\Gamma_{ij} = \gamma_{ij}^2 |F_{ij}(\vec{q})|^2 S_p(\vec{q}) \tag{10}$$

where $S_p(\vec{q})$ denotes the phase space and $F_{ij}(\vec{q})$ are form factors appropriate to exclusive two body decays. Here we have followed ref. [2] and have chosen

$$|F_{ij}(\vec{q})|^2 = q^{2l} exp(-q^2/8\beta^2) \tag{11}$$

where l is the angular momentum of the final state with daughter momenta q and we have used $\beta = 0.5$ GeV/c [2]. The $f_0(1500)$ lies very near to threshold in the $\eta\eta'$ decay mode, therefore we have used an average value of q (190 MeV/c) derived from a fit to the $\eta\eta'$ mass spectrum.

The branching ratios measured by the WA102 experiment for the $f_0(1370)$, $f_0(1500)$ and $f_0(1710)$ are given in table 1.

For quarkonium states the invariant couplings are dependent on the flavour mixing angle $|Q\bar{Q}\rangle \equiv \cos\theta|N\rangle - \sin\theta|S\rangle$. Figs. 2, 3 and 4 show a plot of the ratio of the invariant couplings as a function of θ for the $f_0(1370)$, $f_0(1500)$ and $f_0(1710)$ respectively. Superimposed on the plot are the measured ratios with the $\pm 1\sigma$ limits shown shaded.

As can be seen it is possible to find a solution for the $f_0(1370)$ and $f_0(1500)$ for small values of θ corresponding to them having a large $N \equiv n\bar{n}$ content. This is already an indication that they cannot both be members of the same $q\bar{q}$ nonet unless further degrees of freedom are present. It could be that the $f_0(1370)$ belongs to a lower multiplet than the $f_0(1500)$ or that it does not exist [12]. Even were either of these the case, there would be need for a partner to the $f_0(1500)$ with $\theta \sim 90^\circ - 110^\circ$. Figure 4 shows that the $f_0(1710)$ does not satisfy this. Thus we can already conclude the following:

(i) The $f_0(1500)$, $f_0(1370)$ data show that if both of these states are real, they cannot be in the same $q\bar{q}$ nonet without further degrees of freedom, such as a glueball.

(ii) The $f_0(1710)$ data demonstrate the need to go beyond a simple $q\bar{q}$ picture at some point or that data need to change.

Performing an elementary SU(3) calculation gives the reduced partial widths in table 2, where $\alpha = (\cos\phi - \sqrt{2}\sin\phi)/\sqrt{6}$, $\beta = (\sin\phi + \sqrt{2}\cos\phi)/\sqrt{6}$, and ϕ is the $q\bar{q}$ $S-N$ mixing angle of η and η'. This mixing angle has been determined primarily from electromagnetic interactions that couple directly to the $q\bar{q}$ content of the η, η' states. The relative importance of glue coupling to η and η' may be determined by gluon-driven processes, such as $\psi \to \gamma\eta(\eta')$, or from theoretical arguments about the coupling of the gluon current to the η' system [21]. These independent methods yield consistent results as follows.

(i) The ratio of ψ radiative widths:

$$\frac{\Gamma(\psi \to \eta'\gamma)}{\Gamma(\psi \to \eta\gamma)} = (\frac{q_{\eta'}}{q_\eta})^3 |\frac{\langle 0|j|\eta'\rangle}{\langle 0|j|\eta\rangle}|^2$$

yields

$$|\frac{g_{\eta'}}{g_\eta}| \equiv |\frac{\langle 0|j|\eta'\rangle}{\langle 0|j|\eta\rangle}| = 2.5 \pm 0.2$$

(ii) Theoretical arguments about the coupling of the gluon current to the η' system [21] give

$$\frac{g_{\eta'}}{g_\eta} = \frac{m^2_{\eta'}}{\sqrt{2}m^2_\eta} = 2.2$$

We then perform a χ^2 fit based on the branching ratios given in table 1, where we have required that the matrix U in eq. (2) is unitary, which applies an additional 6 constraints to the fit. As input we use the masses of the $f_0(1500)$ and $f_0(1710)$. In this way the nine parameters, M_G, M_N, M_S, M_3, f, r_2, r_3, r and ϕ are determined from the fit. The mass of the $f_0(1370)$ is not well established so we have left it as a free parameter (M_3).

3.1 Flavour-Blind Glueball

The parameters determined from the fit are given in table 3 and the fitted branching ratios together with the χ^2 contributions of each are given in table 1. Two robust features merit immediate comment. As can be seen the fit prefers a value of $r \approx 1$, in line with the result of Lattice QCD [8]. The mixing angles for the η, η' were unconstrained and the fit chooses the canonical value of -19^o, in agreement with results from elsewhere. The resulting flavour content of the mixed states is

$$\begin{array}{lccc} & f_{i1}^{(G)} & f_{i2}^{(S)} & f_{i3}^{(N)} \\ f_0(1710) & 0.39 & 0.91 & 0.14 \\ f_0(1500) & -0.69 & 0.34 & -0.63 \\ f_0(1370) & -0.62 & 0.13 & 0.77 \end{array} \tag{12}$$

This matrix confirms the robustness of the qualitative pattern that had followed from the mass matrix analyses, namely two states with a singlet tendency and one with an octet. Although these relative phases appear to be stable, the relative intensities of G and flavours differ; the $m_G \sim 1440 \pm 10$ MeV is in the lower end of the mass range preferred by some reports from Lattice-QCD [1], while rather lower than the preferred solution of ref. [8]. Consequently the leading structure of the mixing pattern follows from degenerate perturbation theory with basis states $S, (N \pm G)/\sqrt{2}$. The structure of eq. 12, and what follows, all show this tendency. We shall discuss the implications of these results in more detail later.

This conclusion following from the decay analysis appears to be stable against changes in the detailed dynamics. As an example we return to the model assumption made in our previous paper [15], namely that the glue couple to the η states in proportion to their $s\bar{s}$ content. The expressions for the partial widths are given in table 4. (In this table we have corrected a sign error that appeared in table 3 of ref. [15])). The results of the fit using these expressions are given in tables 5 and 6. The χ^2 of the fit is 13.7 which is worse that the value obtained from the previous fit but the structure essentially remains unchanged:

$$\begin{array}{lccc} & f_{i1}^{(G)} & f_{i2}^{(S)} & f_{i3}^{(N)} \\ f_0(1710) & 0.42 & 0.89 & 0.16 \\ f_0(1500) & -0.64 & 0.37 & -0.67 \\ f_0(1370) & -0.63 & 0.15 & 0.76 \end{array} \tag{13}$$

The general conclusion appears to be that analysis of decays of these scalars reveals the same qualitative pattern of mixing phases as deduced in the mass mixing analyses. The most general interpretation is that these three states are mixed by a flavour singlet coupling: a glueball is a particular example of this. While this does not prove that the glueball is responsible, the robustness of the results, and the implications of lattice QCD that such a state should exist in this mass range, are strongly suggestive.

3.1.1 Insensitivity to choice of data sets

To date we have used the branching ratios measured by experiment WA102 since this is the only experiment in the world to have measured all the ratios. However, the branching ratios have in part been measured by other experiments. Crystal Barrel [22] have presented ratios for the $f_0(1370)$ and $f_0(1500)$. BES have produced a measurement of the $\pi^+\pi^-/KK$ ratio for the $f_0(1370)$ [23] and there are measurements of the $\pi^+\pi^-/KK$ ratio for the $f_0(1710)$ from experiments WA76 [24] and Mark III [25]. It is important to note that these other measured values are compatible with the ones measured by experiment WA102.

We have calculated the world average branching ratios for the $f_0(1370)$, $f_0(1500)$ and the $f_0(1710)$ using all the available data. The values are given in table 7. We have performed a fit to these values using our formula and with r = 1 and ϕ = -19 degrees. The parameters from the fit are given in table 8.

The mixed states are

$$\begin{array}{lccc} & f_{i1}^{(G)} & f_{i2}^{(S)} & f_{i3}^{(N)} \\ f_0(1710) & 0.42 & 0.89 & 0.16 \\ f_0(1500) & -0.66 & 0.37 & -0.64 \\ f_0(1370) & -0.61 & 0.14 & 0.78 \end{array} \tag{14}$$

and the $\chi^2 = 14$. These are identical within the errors to the results that followed from the fit to the WA102 data alone.

3.1.2 Widths

Anisovich [5] has argued that a signature of a glueball driven mixing will be the presence of two states that are narrow and one that is broad. This result would arise if the flavour singlet channels that drive

the mixing, also dominate the physical hadron states (in which case the "octet" will be narrow due to decoupling, the "glue + singlet" enhanced by constructive interference while the "glue − singlet" will be suppressed by destructive interference), but it is less clear in a dynamics such as we have considered here. The analyses of section 3 and 3.1 do have implications for the relative sizes of the total widths of the scalars for decays into pseudoscalar pairs. A consistency check on these results should take account of this; that is the purpose of this subsection.

The measured widths for the $f_0(1370)$, $f_0(1500)$ and $f_0(1710)$ are $272 \pm 40 \pm 30$ MeV, $108 \pm 14 \pm 12$ MeV and $124 \pm 16 \pm 18$ MeV respectively [14]. Based on the observed decay modes of these states [14] and taking into account the uncertainty in possible $\rho\rho$ modes, which would also imply the presence of $\omega\omega$ decay modes, the sums of the partial widths to pseudoscalar pairs are:

$$f_0(1370) = 12 \pm 5 \text{ MeV}; f_0(1500) = 56 \pm 8 \text{ MeV}; f_0(1710) = 124\ ^{+16}_{-50}\text{MeV}$$

If in addition to the analysis of section 3.1 we constrain the ratios of the observed total widths into pseudoscalar pairs, then we find an acceptable fit such that

$$\frac{\Gamma(1710)}{\Gamma(1370)} = 7.1 \pm 2.2; \frac{\Gamma(1500)}{\Gamma(1370)} = 10.0 \pm 3.0; \frac{\Gamma(1710)}{\Gamma(1500)} = 0.7 \pm 0.2$$

which are compatible with the empirical values above. Performing a fit to the measured branching fractions gives the parameters in table 1 and 3.

As can be seen, adding the constraint of the ratio of the total widths makes the M_N and M_G come very close together

$$M_G = 1415 \text{ MeV}; M_S = 1677 \text{ MeV}; M_N = 1402 \text{ MeV}$$

the mixed states are

$$
\begin{array}{lccc}
 & f_{i1}^{(G)} & f_{i2}^{(S)} & f_{i3}^{(N)} \\
f_0(1710) & 0.35 & 0.93 & 0.13 \\
f_0(1500) & -0.61 & 0.29 & -0.74 \\
f_0(1370) & -0.76 & 0.16 & 0.63
\end{array}
\qquad (15)
$$

and the $\chi^2 = 10$.

There is an immediate physical reason for the pattern that emerges in eq. (15), namely the proximity of $m_G \sim m_N$. In this case the parameters have the values $\xi > 1$ whereas $\xi\omega \sim 1/3$. Thus mixing in the $G - N$ sector tends to be maximal (analogous to eq. (7) or eq. (9)) and the structure of the mixed states will tend towards

$$
\begin{array}{lccc}
 & f_{i1}^{(G)} & f_{i2}^{(S)} & f_{i3}^{(N)} \\
f_0(1710) & O(\xi\omega) & 1 & O(\sqrt{2}(\xi\omega)^2) \\
f_0(1500) & -\sqrt{1/3} & O(\xi\omega) & -\sqrt{2/3} \\
f_0(1370) & -\sqrt{2/3} & O(\xi\omega) & \sqrt{1/3}
\end{array}
\qquad (16)
$$

This structure is common to eq. (15) and indeed all of the mixing patterns found throughout section 3.1 where the decay data constraints have been imposed. The central message of the decay data is that they prefer $m_G \sim m_N$. m_G nonet with

3.2 Flavour dependent $G \to q\bar{q}$

3.2.1 $m_G > m_S$

Our analysis of decays has pointed towards a $G - q\bar{q}$ coupling that is approximately flavour independent, and a $m_G < \frac{m_S + m_N}{2}$. This is in contrast to the analysis in ref. [8] which preferred $m_S > m_G$. In this section we ask what flavour dependence of G decays would be required for the latter solution to emerge.

If we write $R \equiv \frac{\gamma(G \to n\bar{n})}{\sqrt{2}\gamma(G \to s\bar{s})}$ then the reduced partial widths are given in table 9.

$R \to 1$ recovers the previous formulae, and initially we set $r_3 = 0$ (i.e. consider only $G \to q\bar{q}$ and ignore any possible additional direct coupling of $G \to \eta, \eta'$). Performing a fit to the measured branching fractions gives the parameters in table 10 and 11.

The best fit (table 10) has $r_2 \sim 5.4$ (which implies that the G dominates the decays) and $R \sim 0.67$ (which implies that G couples more strongly to $s\bar{s}$ than to $n\bar{n}$). This is what is required, at least within the decay dynamics that we have assumed in this paper, if the mass matrix solution of ref. [8] is to be consistent with the decay data. However, we note that the $\chi^2 = 80$. The major mismatches between fit and data are driven by $f_0(1710) \to \pi\pi/K\bar{K}$;

$f_0(1710) \to \eta\eta'/K\bar{K}$ and some from $f_0(1500) \to \eta\eta'/\eta\eta$. A challenge for future data will be to determine the accuracy of these critical branching ratios.

We have investigated whether these conclusions are radically altered if we allow r_3 to be free (i.e. allow additional direct coupling of $G \to \eta\eta'$). These results also are given in tables 10 and 11. The χ^2 falls to 19 and is significantly driven by the $K\bar{K}/\pi\pi$ ratio being smaller (larger) than data for the $f_0(1500)$ ($f_0(1370)$) respectively. $R \sim 0.5$ which still implies a significant favouring of G coupling to the heavier flavoured S rather than N. With the advent of more powerful studies of QCD on the lattice, it will be interesting to see if such behaviour is realised. However, the χ^2 is much larger than the value of 5.4 that was found for the solution of table 1, eq. (12) and section 3.1.

3.2.2 Light Glueball: $m_G < m_N$

In concluding our studies of flavour dependent G couplings, we note that if we allow the bare masses to be free and keep $r_3 = 0$, then there exists a solution ($\chi^2 = 13$) with $R = 1.4 \pm 0.4$, for which the mass of the bare glueball is $m_G = 1310 \pm 14$MeV . See tables 12 and 13. The mixing matrix has the generic structure exhibited in eq. (16), modulated by the G, N tending to settle into the $f_0(1370)$ and $f_0(1500)$ states. Explicitly it is

$$\begin{array}{cccc} & f_{i1}^{(G)} & f_{i2}^{(S)} & f_{i3}^{(N)} \\ f_0(1710) & 0.25 & 0.96 & 0.10 \\ f_0(1500) & -0.37 & 0.13 & -0.92 \\ f_0(1370) & -0.89 & 0.14 & 0.44 \end{array} \tag{17}$$

We do not discuss this further here, other than to note that it implies that a light glueball may be compatible with data. Furthermore, it is tantalising that such a result could be in accord with Lattice QCD (see for example the results with coarse lattices in ref. [6]). If such a result should emerge from future studies of QCD with fine grain lattices and including mixing then a detailed analysis of the phenomenology along the lines we have instigated here would be most interesting. We leave this as a future challenge for Lattice QCD.

If we then allow r_3 to be a free parameter we get a χ^2 of 6.7. The results are given in tables 12 and 13. In this case M_G is tending towards M_N and the solution is similar to the one we obtain in tables 1 and 3. The mixing matrix naturally shows the form of eq. (16).

We note that $m_G \sim 1402$ MeV is only slightly lower than $m_N \sim 1446$ MeV and the result is not dissimilar to that preferred in section 3.1. However, in both the cases $m_G > m_S$ and $m_G < m_N$ there is a clear omission, namely of mixing with nearest neighbour states above the glueball when $m_G > m_S$, (section 3.2.1), or below it when $m_N < m_G$, (section 3.2.2). Therefore, if m_G should indeed turn out to be $< m_N$, further analysis should be required involving the $f_0(980)$ region, or the $\pi\pi$ $S-$wave continuum below 1 GeV [26].

4 Result

Given the concerns expressed above about the $m_G > m_S$ and $m_G < m_N$ scenarios, it is the results of section 3.1 that are our preferred solution. With the hypotheses that the mixing describe the ratios of partial widths for each individual resonance and also among the resonances, we take into account the variability between WA102 data and world averages, and we allow for the uncertainties in flavour dependence of the glueball coupling. This gives our final result, based on eqs. (12, 14, 15), as follows.

$$\begin{array}{cccc} & f_{i1}^{(G)} & f_{i2}^{(S)} & f_{i3}^{(N)} \\ f_0(1710) & 0.39 \pm 0.03 & 0.91 \pm 0.02 & 0.15 \pm 0.02 \\ f_0(1500) & -0.65 \pm 0.04 & 0.33 \pm 0.04 & -0.70 \pm 0.07 \\ f_0(1370) & -0.69 \pm 0.07 & 0.15 \pm 0.01 & 0.70 \pm 0.07 \end{array} \qquad (18)$$

and for which $m_G = 1443 \pm 24$ MeV, $m_N = 1377 \pm 20$ MeV

and $m_S = 1674 \pm 10$ MeV.

The specific numbers in the above matrix correlate with the specific values of $m_{G,N,S}$ but the generic structure shows the form of eq. (16). Physically this reflects the dominant flavour-blind nature of the $G - q\bar{q}$ coupling, amplified by the proximity of $m_G \sim m_N$ whereas $m_G \neq m_S$. In the degenerate limit of $m_G \to m_N$, the mixing would indeed tend towards that in eq. (16).

5 Further Tests

5.1 $\gamma\gamma$ couplings

The most sensitive probe of flavours and phases is potentially in $\gamma\gamma$ couplings. The advantage is that $\gamma\gamma$ couple to the e^2 of the flavours in amplitude and so the net result is sensitive to the relative phases as well as the intensities. That this is a dominant dynamics is empirically well established for the 2^{++} and 0^{-+} nonets; however it is moot whether it will in fact be so clean for the 0^{++}. If it is dominant for this J^{PC} also, then in the spirit of ref. [7], ignoring mass-dependent effects, the above imply

$$\Gamma(f_0(1710) \to \gamma\gamma) : \Gamma(f_0(1500) \to \gamma\gamma) : \Gamma(f_0(1370) \to \gamma\gamma) = (5z_1 + \sqrt{2}y_1)^2 : (5z_2 + \sqrt{2}y_2)^2 : (5z_3 + \sqrt{2}y_3)^2 \qquad (19)$$

For the case of the flavour blind glueball given in section 3.1 we get two predictions for these relationships: one for the case when we do not add the total widths as a constraint and one when we do. We have averaged these two values and used their difference as a measure of the systematic error

$$\Gamma^{\gamma\gamma}(f_0(1710) : f_0(1500) : f_0(1370)) = 4.1 \pm 0.9 \pm 0.3 : 9.7 \pm 0.9 \pm 2.0 : 14.6 \pm 0.9 \pm 2.0 \qquad (20)$$

The $\gamma\gamma$ width of $f_0(1500)$ exceeding that of $f_0(1710)$ arises because the glueball is nearer to the N than the S. The pattern is radically different if nature chooses G near to (or even above) the S, in which case the $f_0(1500)$ has the smallest $\gamma\gamma$ coupling of the three states [7]. For example, in the case of flavour dependent mixing with $M_G > M_S$ (section 3.2.1) we find

$$\Gamma^{\gamma\gamma}(f_0(1710) : f_0(1500) : f_0(1370)) = 6.4 \pm 1.1 : 0.6 \pm 0.2 : 23.8 \pm 2.2 \tag{21}$$

Contrast this with the case of flavour dependent mixing with $M_G < M_N$ (section 3.2.2) for which

$$\Gamma^{\gamma\gamma}(f_0(1710) : f_0(1500) : f_0(1370)) = 3.2 \pm 1.1 : 16.3 \pm 1.8 : 9.0 \pm 0.8 \tag{22}$$

This shows how these $\gamma\gamma$ couplings have the potential to pin down the input pattern. However, we note a caution with regards to $\gamma\gamma$ couplings necessarily being the arbiter on $G - q\bar{q}$ wavefunctions in the 0^{++} partial waves. A problem here is that 0^{++} states decay to meson pairs in S-wave (this is kinematically forbidden for the low-lying 0^{-+} or 2^{++} nonets) and so meson loops may be expected to intercede between the $\gamma\gamma$ and $q\bar{q}$ levels. Insights from $\gamma\gamma \to f_0(980)/a_0(980)$, from models and ultimately from lattice QCD will be needed to establish how clean in practice the $\gamma\gamma$ measurements can be in the 0^{++} sector.

5.2 Glue and Pomeron induced reactions: Central Production

Our preferred solutions have two further implications for the production of these states in $p\bar{p}$ annihilations, in central pp collisions and in radiative J/ψ decays that are in accord with data. These are interesting in that they are consequences of the output and were not used as constraints.

The production of the f_0 states in $p\bar{p} \to \pi + f_0$ is expected to be dominantly through the $N \equiv n\overline{n}$ components of the f_0 state, possibly through G, but not prominently through the $S \equiv s\overline{s}$ components. (The possible presence of hidden $s\overline{s}$ at threshold, noted by [27] is in general swamped by the above, and in any event appears unimportant in flight). The above mixing pattern implies that

$$\sigma(p\overline{p} \to \pi + f_0(1710)) < \sigma(p\overline{p} \to \pi + f_0(1370)) \sim \sigma(p\overline{p} \to \pi + f_0(1500)) \tag{23}$$

Experimentally [28] the relative production rates are,

$$p\overline{p} \to \pi + f_0(1370) : \pi + f_0(1500)) \sim 1 : 1. \tag{24}$$

and there is no evidence for the production of the $f_0(1710)$. This would be natural if the production were via the $n\overline{n}$ component. The actual magnitudes would however be model dependent; at this stage we merely note the consistency of the data with the results of the mixing analysis above.

For central production, the cross sections of well established quarkonia in WA102 suggest that the production of $s\overline{s}$ is strongly suppressed [29] relative to $n\overline{n}$. The relative cross sections for the three states of interest here are

$$pp \to pp + (f_0(1710) : f_0(1500) : f_0(1370)) \sim 0.14 : 1.7 : 1. \qquad (25)$$

This would be natural if the production were via the N and G components in phase.

In addition, the WA102 collaboration has studied the production of these states as a function of the azimuthal angle ϕ, which is defined as the angle between the p_T vectors of the two outgoing protons. An important qualitative characteristic of these data is that the $f_0(1710)$ and $f_0(1500)$ peak as $\phi \to 0$ whereas the $f_0(1370)$ is more peaked as $\phi \to 180$ [30]. If the G and N components are produced coherently as $\phi \to 0$ but out of phase as $\phi \to 180$, then this pattern of ϕ dependence and relative production rates would follow; however, the relative coherence of G and N requires a dynamical explanation. We do not have such an explanation and open this for debate.

In J/ψ radiative decays, the absolute rates depend sensitively on the phases and relative strengths of the G relative to the $q\overline{q}$ component, as well as the relative phase of $n\bar{n}$ and $s\bar{s}$ within the latter. The general pattern though is clear. Following the discussion in ref. [7] we expect that the coupling to G will be large; coupling to $q\bar{q}$ with "octet tendency" will be suppressed; coupling to $q\bar{q}$ with "singlet tendency" will be intermediate. Hence the rate for $f_0(1370)$ will be smallest as the G interferes destructively against the $q\bar{q}$ with "singlet tendency". Conversely, the $f_0(1710)$ is enhanced by their constructive interference. The $f_0(1500)$ contains $q\bar{q}$ with "octet tendency" and its production will be driven dominantly by its G content. If the G mass is nearer to the N than to the S, as our results suggest, the G component in $f_0(1500)$ is large and causes the $J/\psi \to \gamma f_0(1500)$ rate to be comparable to $J/\psi \to \gamma f_0(1710)$.

In ref. [25], the branching ratio of $\mathrm{BR}(J/\psi \to \gamma f_0)(f_0 \to \pi\pi + K\bar{K})$ for the $f_0(1500)$ and $f_0(1710)$ is presented. Using the WA102 measured branching fractions [14] for these resonances and assuming that all major decay modes have been observed, the total relative production rates in radiative J/ψ decays can be calculated to be:

$$J/\psi \to f_0(1500) : J/\psi \to f_0(1710) = 1.0 : 1.1 \pm 0.4 \qquad (26)$$

which is consistent with the prediction above based on our mixed state solution.

In these mixed state solutions, both the $f_0(1500)$ and $f_0(1710)$ have N and S contributions and so it would be expected that both would be produced in $\pi^- p$ and $K^- p$ interactions. The $f_0(1500)$ has clearly been observed in $\pi^- p$ interactions: it was first observed in the $\eta\eta$ final state, although at that time it was referred to as the $G(1590)$ [31]. There is also evidence for the production of the $f_0(1500)$ in $K^- p \to K^0_S K^0_S \Lambda$ [32, 33]. The signal is much weaker compared to the well known $s\bar{s}$ state the $f_2'(1525)$, as expected with our preferred mixings in eq. 18 and the suppressed $K\bar{K}$ decay associated with the destructive $n\bar{n} - s\bar{s}$ phase in the wavefunction.

There is evidence for the $f_0(1710)$ in the reaction $\pi^- p \to K^0_S K^0_S n$, originally called the $S^{*\prime}(1720)$ [34, 35]. One of the longstanding problems of the $f_0(1710)$ is that in-spite of its dominant $K\bar{K}$ decay mode it was not observed in $K^- p$ experiments [33, 36]. However, these concerns were based on the fact that initially the $f_0(1710)$ had $J = 2$. In fact, in ref. [37] it was demonstrated that if the $f_0(1710)$ had $J = 0$, as it has now been found to have, then the contribution in $\pi^- p$ and $K^- p$ are compatible. One word of caution should be given here: the analysis in ref. [37] was performed with a $f_0(1400)$ rather than the $f_0(1500)$ as we know it today. As a further test of our solution, it would be nice to see the analysis of ref. [37] repeated with the mass and width of the $f_0(1500)$ and the decay parameters of the $f_0(1710)$ determined by the WA102 experiment.

6 Conclusions

We took as our guide the prediction of Lattice-QCD that, in the quenched approximation, $m_G(0^{++}) \sim 1.5$ GeV, and we explored the implications of the hypothesis that this glueball mixes with its nearest $q\bar{q}$ neighbours. This led us naturally to focus on the physical states the $f_0(1370)$, $f_0(1500)$ and $f_0(1710)$. This has been the philosophy behind several recent analyses, which appear different in detail at first sight, but which turn out to have certain robust common features. We have abstracted these and specified the critical data that are now required to make further progress.

The first studies of mixing were based on the mass matrix and the assumption that the glueball-$q\bar{q}$ mixing is dominantly singlet in character. The resulting output of two states that have constructive interference "singlet tendency" and one that has destructive "octet tendency" is then general. This can be seen as a common feature of [2, 8, 9].

The absolute values of the flavour content are correlated with the assumed masses of the bare glueball and quarkonium states. Weingarten's initial work on the lattice assumed that the glueball was higher in mass than the $s\bar{s}$ member of the nonet; this led to a large glueball component in the heaviest state, the $f_0(1710)$ - eq. (5) and a large $s\bar{s}$ content for the $f_0(1500)$. Close and Amsler in contrast assumed that the glueball was initially at a mass spanned by the nonet. This led to a different apportioning of the glue among the states, eq. (6), in particular the G and $s\bar{s}$ have similar intensities in $f_0(1500)$ and $f_0(1710)$.

Subsequent work has also considered the decays into pseudoscalar pairs. The qualitative features of the mixing are preserved, essentially due to the assumed singlet dominance of the (glueball) mixing. A general feature of these later works has been the assumption that the glueball component of the wavefunctions has flavour independent couplings; any deviation from this in the decays of the physical states is then due to the glueball-flavour mixed eigenstates.

A common feature of the various solutions in eqs. (5,6,12) and (15) is

(1) the $f_0(1370)$ has large $n\bar{n}$, small $s\bar{s}$ and significant G content

(2) the $f_0(1710)$ has a large $s\bar{s}$ content in all except Weingarten (eq. (5)) whose solution instead has a large G

(3) $f_0(1500)$,as the central member of the trio, has $s\bar{s}$ and $n\bar{n}$ out of phase.

The decay analyses, eqs. (12) and (15) do show a systematic shift relative to the original mass matrix analyses, eqs. (5) and (6). This appears in two noticeable ways:

(1) The decay analyses want more S in the $f_0(1700)$ and more G in the $f_0(1370)$. This is correlated to them wanting a rather light G mass, whereby the G mixes primarily with N,

leaving the "distant" $f_0(1700)$ as S in leading order with a 10-20 % G intensity.

(2) A corollary is that the S content of the $f_0(1500)$ tends to be driven smaller by the decay analyses. This is in marked contrast to Weingarten where the S content of the $f_0(1500)$ dominates, driven by the nearness of $M_{s\bar{s}}$ to the physical eigenstate in his solution.

Therefore, if the G decay is intrinsically flavour-blind, the results of the decay analyses would imply that the G is rather light, nearer to the N than to the S. This is radically different to Weingarten's assumption that $m_G > m_S > m_N$. The latter requires, within the assumptions of our analysis, that G couples to S more strongly than to N, and also that the coupling of $G \to$ meson pairs is stronger than $Q\bar{Q}$ to the same meson pairs. This latter result appears unnatural to us. It will be a challenge to lattice QCD to study these couplings to see if there is any sign of such unexpected behaviour. In the absence of such an anomaly, we anticipate that the likely inference of this analysis is that G is rather light, nearer to N than to S.

With the hypotheses that the mixing describe the ratios of partial widths for each individual resonance and also among the resonances, allowing for variability between WA102 data and world averages, and allowing for the uncertainties in flavour dependence of the glueball coupling, the results of section 3 lead us to the following summary for the favoured result:

$$\begin{array}{cccc} & f_{i1}^{(G)} & f_{i2}^{(S)} & f_{i3}^{(N)} \\ f_0(1710) & 0.39 \pm 0.03 & 0.91 \pm 0.02 & 0.15 \pm 0.02 \\ f_0(1500) & -0.65 \pm 0.04 & 0.33 \pm 0.04 & -0.70 \pm 0.07 \\ f_0(1370) & -0.69 \pm 0.07 & 0.15 \pm 0.01 & 0.70 \pm 0.07 \end{array} \tag{27}$$

for which $m_G = 1443 \pm 24$ MeV, $m_N = 1377 \pm 20$ MeV and $m_S = 1674 \pm 10$ MeV.

We make two further comments about this result.

(i) In the quenched approximation one would expect an a_0 state that is mass degenerate with the N state before any mixing. Hence we would expect the a_0 to be in this region of $1350 - 1400$ MeV. The existence and mass of any a_0 other than the $a_0(980)$ is still controversial and we advertise this as an important datum that could further constrain analyses such as those we have made in this paper. The presence or absence of an a_0 in the mass region favoured by us could have implications for the interpretation of the $a_0(980)$ and $f_0(980)$ states. Establishing the status of $a_0(\sim 1400)$ should be a high priority in the quest to understand the nature of the 0^{++} mesons.

(ii) We also note that our result that $m_S - m_N \sim 300$ MeV is consistent with what one would expect from $f_2(1525) - f_2(1270)$ or, equivalently, the naive accounting of masses for constituent quarks where $2m_s - 2m_n \sim 0.3$ GeV.

In summary, based on the hypothesis that the scalar glueball mixes with the nearby $q\overline{q}$ nonet states, we have determined the flavour content of the $f_0(1370)$, $f_0(1500)$ and $f_0(1710)$ by studying their decays into all pseudoscalar meson pairs. It suggests that the m_G is relatively light, nearer in mass to m_N than m_S. The solution we have found is also compatible with the relative production strengths of the $f_0(1370)$, $f_0(1500)$ and $f_0(1710)$ in pp central production, $p\bar{p}$ annihilations and J/ψ radiative decays.

Acknowledgements

We are indebted to C. Michael and M. Teper for discussions on glueballs and mixing in lattice QCD. This work is supported, in part, by grants from the British Particle Physics and Astronomy Research Council, the British Royal Society, and the European Community Human Mobility Program Eurodafne, contract NCT98-0169.

References

[1] G. Bali *et al.* (UKQCD), Phys. Lett. **B309** (1993) 378; Phys.Rev. **D62** (2000) 054503.

D. Weingarten, hep-lat/9608070;

J. Sexton et al., Phys. Rev. Lett. **75** (1995) 4563;

F.E. Close and M.J. Teper, "On the lightest Scalar Glueball" Rutherford Appleton Laboratory report no. RAL-96-040; Oxford University report no. OUTP-96-35P

W. Lee and D. Weingarten, hep-lat/9805029

G. Bali hep-ph/0001312

[2] C. Amsler and F.E. Close Phys. Lett. **B353** (1995) 385.

[3] C. Amsler and F.E. Close Phys. Rev. **D53** (1996) 295

[4] N. Isgur and J. Paton, Phys Rev **D31** (1985) 2910.

[5] V.V. Anisovich, Physics-Uspekhi **41** (1998) 419

[6] C. Mc Neile and C. Michael hep-lat/0010019

[7] F.E. Close, G. Farrar and Z.P. Li, Phys.Rev. **D55** (1997) 5749.

[8] W. Lee and D. Weingarten, Phys. Rev. **D 61** (2000) 01405;

D. Weingarten, Nucl. Phys. Proc. Suppl. **53** (1997) 232; **63** (1998) 194;**73** (1999) 249.

[9] De-Min Li, Hong Yu and Qi-Xing Shen, hep-ph/0001107.

[10] M. Genovese, Phys. Rev. **D46** (1992) 5204

[11] D.E. Groom *et al.,* Particle Data Group, European Physical Journal **C15** (2000) 1.

[12] E. Klempt, PSI proceedings, 00-01 (2000) 61. Summer School 2000

[13] A. Kirk, Phys. Lett. **B489** (2000) 29.

[14] D. Barberis *et al.,* Phys. Lett. **B479** (2000) 59.

[15] F.E. Close and A. Kirk, Phys. Lett. **B483** (2000) 345.

[16] F.E. Close, Acta Physica Polonica **B31** (2000) 2557

[17] P.Lacock et al. (UKQCD Collaboration), Phys.Rev. **D54** (1996) 6997

[18] D.M. Li, H. Yu and Q.X. Shen, hep-ph/0011129

[19] N. Isgur and J. Paton, Phys. Rev. **D31** (1985) 2910.

[20] S.S. Gershtein *et al.,* Zeit. Phys. **C24** (1984) 305. 4157

[21] V.A. Novikov *et al.,* Nucl. Phys. **B165** (1980) 55.

[22] Crystall Barrel paper submitted to EPJ

[23] D.Bugg (private communication; BES in preparation)

[24] T.A. Armstrong *et al.,* Zeit. Phys. **C51** (1991) 351.

[25] W. Dunwoodie, Proceedings of HAdron 97, AIP Conf. Series 432 (1997) 753.

[26] P. Minkowski and W. Ochs, Eur.Phys.J **C9** (1999) 283.

[27] J. Ellis, E. Gabathuler and M. Karliner, Phys. Lett. **B217** (1989) 173.

[28] U. Thoma, Proceedings of Hadron 99, Beijing, China 1999.

[29] D. Barberis *et al.,* Phys. Lett. **B462** (1999) 462.

[30] D. Barberis *et al.,* Phys. Lett. **B467** (1999) 165.

[31] F. Binon *et al.,* Il Nuovo Cimento **A78** (1983) 313.

[32] M. Baubillier *et al.,* Zeit. Phys. **C17** (1983) 309.

[33] D. Aston *et al.,* Nucl. Phys. **B301** (1988) 525.

[34] A. Etkin *et al.,* Phys. Rev. **D25** (1982) 1786.

[35] B.V. Bolonkin *et al.,* AIP. Conf. Proc. 185 (1988) 289.

[36] Ph. Gavillet *et al.,* Zeit. Phys. **C16** (1982) 119.

[37] S. Lindenbaum and R.S. Longacre, Phys. Lett. **B274** (1992) 492.

Table 1: The solutions for the minimum χ^2 (total width constraint).

	Measured Branching ratio	new formula r free Fitted	χ^2	new formula r free width cons Fitted	χ^2
$\frac{f_0(1370)\rightarrow\pi\pi}{f_0(1370)\rightarrow K\overline{K}}$	2.17 ± 0.9	2.14	0.001	0.38	3.97
$\frac{f_0(1370)\rightarrow\eta\eta}{f_0(1370)\rightarrow K\overline{K}}$	0.35 ± 0.21	0.41	0.08	0.42	0.13
$\frac{f_0(1500)\rightarrow\pi\pi}{f_0(1500)\rightarrow\eta\eta}$	5.5 ± 0.84	5.79	0.12	5.7	0.06
$\frac{f_0(1500)\rightarrow K\overline{K}}{f_0(1500)\rightarrow\pi\pi}$	0.32 ± 0.07	0.38	0.65	0.43	2.5
$\frac{f_0(1500)\rightarrow\eta\eta'}{f_0(1500)\rightarrow\eta\eta}$	0.52 ± 0.16	0.50	0.02	0.55	0.02
$\frac{f_0(1710)\rightarrow\pi\pi}{f_0(1710)\rightarrow K\overline{K}}$	0.20 ± 0.03	0.18	0.43	0.19	0.10
$\frac{f_0(1710)\rightarrow\eta\eta}{f_0(1710)\rightarrow K\overline{K}}$	0.48 ± 0.14	0.20	4.08	0.24	2.90
$\frac{f_0(1710)\rightarrow\eta\eta'}{f_0(1710)\rightarrow\eta\eta}$	$< 0.05(90\% cl)$	0.04	0.06	0.03	0.05

Table 2: The theoretical reduced partial widths (new formula).

$\gamma^2(f_i \to \eta\eta')$	$2[2\alpha\beta(z_i - \sqrt{2}y_i) + 2\frac{g_{\eta'}}{g_\eta}x_i r_3]^2$
$\gamma^2(f_i \to \eta\eta)$	$[2\alpha^2 z_i + 2\sqrt{2}\beta^2 y_i + r_2 x_i + 2x_i r_3]^2$
$\gamma^2(f_i \to \pi\pi)$	$3[z_i + r_2 x_i]^2$
$\gamma^2(f_i \to K\bar{K})$	$4[\frac{1}{2}(z_i + \sqrt{2}y_i) + r_2 x_i]^2$

Table 3: The solutions for the minimum χ^2 new formula.

Parameters	r free	r free width cons
χ^2	5.4	10.1
M_G (MeV)	1441 ± 12	1415 ± 16
M_S (MeV)	1675 ± 9	1680 ± 12
M_N (MeV)	1364 ± 19	1405 ± 22
M_3 (MeV)	1264 ± 14	1265 ± 18
f (MeV)	85 ± 10	85 ± 12
ϕ (Deg)	-19 ± 3	-15 ± 5
r_2	0.96 ± 0.26	1.21 ± 0.29
r_3	0.09±0.03	0.15±0.04
r	1.0± 0.3	0.96± 0.3

Table 4: The theoretical reduced partial widths (old formula corrected).

$\gamma^2(f_i \to \eta\eta')$	$2[2\alpha\beta(z_i - \sqrt{2}y_i) - 2\alpha\beta x_i r_3]^2$
$\gamma^2(f_i \to \eta\eta)$	$[2\alpha^2 z_i + 2\sqrt{2}\beta^2 y_i + r_2 x_i + 2\beta^2 x_i r_3]^2$
$\gamma^2(f_i \to \pi\pi)$	$3[z_i + r_2 x_i]^2$
$\gamma^2(f_i \to K\bar{K})$	$4[\frac{1}{2}(z_i + \sqrt{2}y_i) + r_2 x_i]^2$

Table 5: The solutions for the minimum χ^2 (old formula).

Parameters	corrected
χ^2	13.7
M_G (MeV)	1438 $\pm$ 12
M_S (MeV)	1667 $\pm$ 10
M_N (MeV)	1370 $\pm$ 19
M_3 (MeV)	1258 $\pm$ 28
f (MeV)	95 $\pm$ 26
ϕ (Deg	-19$\pm$ 2
r_2	0.94 $\pm$ 0.09
r_3	0.40$\pm$ 0.30

Table 6: The measured and predicted branching ratios with the individual χ^2 contributions coming from the fits.

	Measured Branching ratio	Old formula corrected Fitted	χ^2
$\frac{f_0(1370)\to\pi\pi}{f_0(1370)\to K\overline{K}}$	2.17 ± 0.9	2.1	0.005
$\frac{f_0(1370)\to\eta\eta}{f_0(1370)\to K\overline{K}}$	0.35 ± 0.21	0.18	0.62
$\frac{f_0(1500)\to\pi\pi}{f_0(1500)\to\eta\eta}$	5.5 ± 0.84	6.5	1.4
$\frac{f_0(1500)\to K\overline{K}}{f_0(1500)\to\pi\pi}$	0.32 ± 0.07	0.32	1.1
$\frac{f_0(1500)\to\eta\eta'}{f_0(1500)\to\eta\eta}$	0.52 ± 0.16	0.17	4.8
$\frac{f_0(1710)\to\pi\pi}{f_0(1710)\to K\overline{K}}$	0.20 ± 0.03	0.2	0.03
$\frac{f_0(1710)\to\eta\eta}{f_0(1710)\to K\overline{K}}$	0.48 ± 0.14	0.19	4.3
$\frac{f_0(1710)\to\eta\eta'}{f_0(1710)\to\eta\eta}$	$< 0.05(90\% cl)$	0.09	2.5

Table 7: Our formula (no total width) world average.

	Measured Branching ratio	all Fitted	χ^2
$\frac{f_0(1370)\to\pi\pi}{f_0(1370)\to K\overline{K}}$	1.78 ± 0.9	2.16	0.18
$\frac{f_0(1370)\to\eta\eta}{f_0(1370)\to K\overline{K}}$	0.11 ± 0.15	0.27	1.1
$\frac{f_0(1500)\to\pi\pi}{f_0(1500)\to\eta\eta}$	7.7 ± 1.5	8.3	0.16
$\frac{f_0(1500)\to K\overline{K}}{f_0(1500)\to\pi\pi}$	0.21 ± 0.05	0.35	7.4
$\frac{f_0(1500)\to\eta\eta'}{f_0(1500)\to\eta\eta}$	0.71 ± 0.13	0.0.56	1.4
$\frac{f_0(1710)\to\pi\pi}{f_0(1710)\to K\overline{K}}$	0.26 ± 0.07	0.21	0.44
$\frac{f_0(1710)\to\eta\eta}{f_0(1710)\to K\overline{K}}$	0.48 ± 0.14	0.0.22	3.5
$\frac{f_0(1710)\to\eta\eta'}{f_0(1710)\to\eta\eta}$	$< 0.05(90\%cl)$	0.05	0.01

Table 8: Our formula (no total width) world average.

Parameters	all ratios
χ^2	14.2
M_G (MeV)	1473 $\pm$ 15
M_S (MeV)	1667 $\pm$ 16
M_N (MeV)	1363 $\pm$ 21
M_3 (MeV)	1258 $\pm$ 33
f (MeV)	94 $\pm$ 16
ϕ (Deg)	-19
r_2	0.99 $\pm$ 0.27
r_3	0.04 $\pm$ 0.02

Table 9: The theoretical reduced partial widths (Weingarten).

$\gamma^2(f_i \to \eta\eta')$	$2[2\alpha\beta(z_i - \sqrt{2}y_i) + x_i r_2(1 - R^{-2}) + 2\frac{g_{\eta'}}{g_\eta} x_i r_3]^2$
$\gamma^2(f_i \to \eta\eta)$	$[2\alpha^2(z_i + x_i r_2) + 2\beta^2(\sqrt{2}y_i + r_2 x_i R^{-2}) + 2x_i r_3]^2$
$\gamma^2(f_i \to \pi\pi)$	$3[z_i + r_2 x_i]^2$
$\gamma^2(f_i \to K\bar{K})$	$4[\frac{1}{2}(z_i + \sqrt{2}y_i) + R^{-1} r_2 x_i]^2$

Table 10: The solutions for the minimum χ^2 (weingartens formula fixed mass $R < 1$).

Parameters	$r_3 = 0$	r_3 free
χ^2	81.7	19.3
M_G (MeV)	1622	1622
M_S (MeV)	1514	1514
M_N (MeV)	1470	1470
M_3 (MeV)	1366	1363
f (MeV)	88 $\pm$ 21	99 $\pm$ 21
ϕ (Deg)	-19	-19
r_2	5.40 $\pm$ 0.94	2.89 $\pm$ 0.40
r_3	0.0	1.08$\pm$ 0.17
R	0.68 $\pm$ 0.16	0.52$\pm$ 0.04

Table 11: Weingarten formula fixed mass $R < 1$

	Measured Branching ratio	r_3 fixed 0 Fitted	χ^2	r_3 free Fitted	χ^2
$\frac{f_0(1370)\to\pi\pi}{f_0(1370)\to K\overline{K}}$	2.17 $\pm$ 0.9	0.34	4.1	0.11	5.2
$\frac{f_0(1370)\to\eta\eta}{f_0(1370)\to K\overline{K}}$	0.35 $\pm$ 0.21	0.19	0.58	0.49	0.43
$\frac{f_0(1500)\to\pi\pi}{f_0(1500)\to\eta\eta}$	5.5 $\pm$ 0.84	6.5	1.41	4.0	3.1
$\frac{f_0(1500)\to K\overline{K}}{f_0(1500)\to\pi\pi}$	0.32 $\pm$ 0.07	0.39	1.00	0.16	5.3
$\frac{f_0(1500)\to\eta\eta'}{f_0(1500)\to\eta\eta}$	0.52 $\pm$ 0.16	0.0003	10.5	0.32	1.5
$\frac{f_0(1710)\to\pi\pi}{f_0(1710)\to K\overline{K}}$	0.20 $\pm$ 0.03	0.39	39.5	0.26	3.6
$\frac{f_0(1710)\to\eta\eta}{f_0(1710)\to K\overline{K}}$	0.48 $\pm$ 0.14	0.22	3.48	0.44	0.09
$\frac{f_0(1710)\to\eta\eta'}{f_0(1710)\to\eta\eta}$	$< 0.05(90\%cl)$	0.18	21.1	0.05	0.003

Table 12: The solutions for the minimum χ^2 (free mass $R > 1$).

Parameters	r_3 Fixed 0	r_3 free
χ^2	12.9	6.7
M_G (MeV)	1310 $\pm$ 14	1402 $\pm$ 12
M_S (MeV)	1692 $\pm$ 16	1694 $\pm$ 13
M_N (MeV)	1460 $\pm$ 23	1446 $\pm$ 18
M_3 (MeV)	1257 $\pm$ 25	1301 $\pm$ 23
f (MeV)	70 $\pm$ 11	66 $\pm$ 10
ϕ (Deg)	-19	-19
r_2	1.69 $\pm$ 0.21	1.91 $\pm$ 0.20
r_3	0.	0.12$\pm$ 0.04
R	1.37$\pm$ 0.38	1.32$\pm$ 0.32

Table 13: free mass $R > 1$

	Measured Branching ratio	r_3 fixed 0 Fitted	r_3 fixed 0 χ^2	r_3 free Fitted	r_3 free χ^2
$\frac{f_0(1370)\to\pi\pi}{f_0(1370)\to K\overline{K}}$	2.17 $\pm$ 0.9	1.72	0.25	1.57	0.44
$\frac{f_0(1370)\to\eta\eta}{f_0(1370)\to K\overline{K}}$	0.35 $\pm$ 0.21	0.30	0.05	0.38	0.05
$\frac{f_0(1500)\to\pi\pi}{f_0(1500)\to\eta\eta}$	5.5 $\pm$ 0.84	7.8	7.7	6.2	0.6
$\frac{f_0(1500)\to K\overline{K}}{f_0(1500)\to\pi\pi}$	0.32 $\pm$ 0.07	0.32	0.005	0.37	0.53
$\frac{f_0(1500)\to\eta\eta'}{f_0(1500)\to\eta\eta}$	0.52 $\pm$ 0.16	0.48	0.06	0.60	0.23
$\frac{f_0(1710)\to\pi\pi}{f_0(1710)\to K\overline{K}}$	0.20 $\pm$ 0.03	0.20	0.0003	0.20	0.0003
$\frac{f_0(1710)\to\eta\eta}{f_0(1710)\to K\overline{K}}$	0.48 $\pm$ 0.14	0.17	4.75	0.20	4.14
$\frac{f_0(1710)\to\eta\eta'}{f_0(1710)\to\eta\eta}$	$< 0.05(90\% cl)$	0.05	0.025	0.05	0.004

Figures

Figure 1: The Decays to Pseudoscalar meson pairs (PP) considered in this analysis. a) The coupling of the $q\bar{q}$ to the PP pair, b) the coupling of the glueball component to PP and c) the direct coupling of gluons to the gluonic component of the final state mesons.

Figure 2: The ratio of the invariant coupling amplitudes squared as a function of the flavour mixing angle θ for the $f_0(1370)$. Superimposed on the plots is the measured ratios. The band indicates the $\pm 1\sigma$ region.

Figure 3: The ratio of the invariant coupling amplitudes squared as a function of the flavour mixing angle θ for the $f_0(1500)$. Superimposed on the plots is the measured ratios. The band indicates the $\pm 1\sigma$ region.

Figure 4: The ratio of the invariant coupling amplitudes squared as a function of the flavour mixing angle θ for the $f_0(1710)$. Superimposed on the plots is the measured ratios. The band indicates the $\pm 1\sigma$ region.

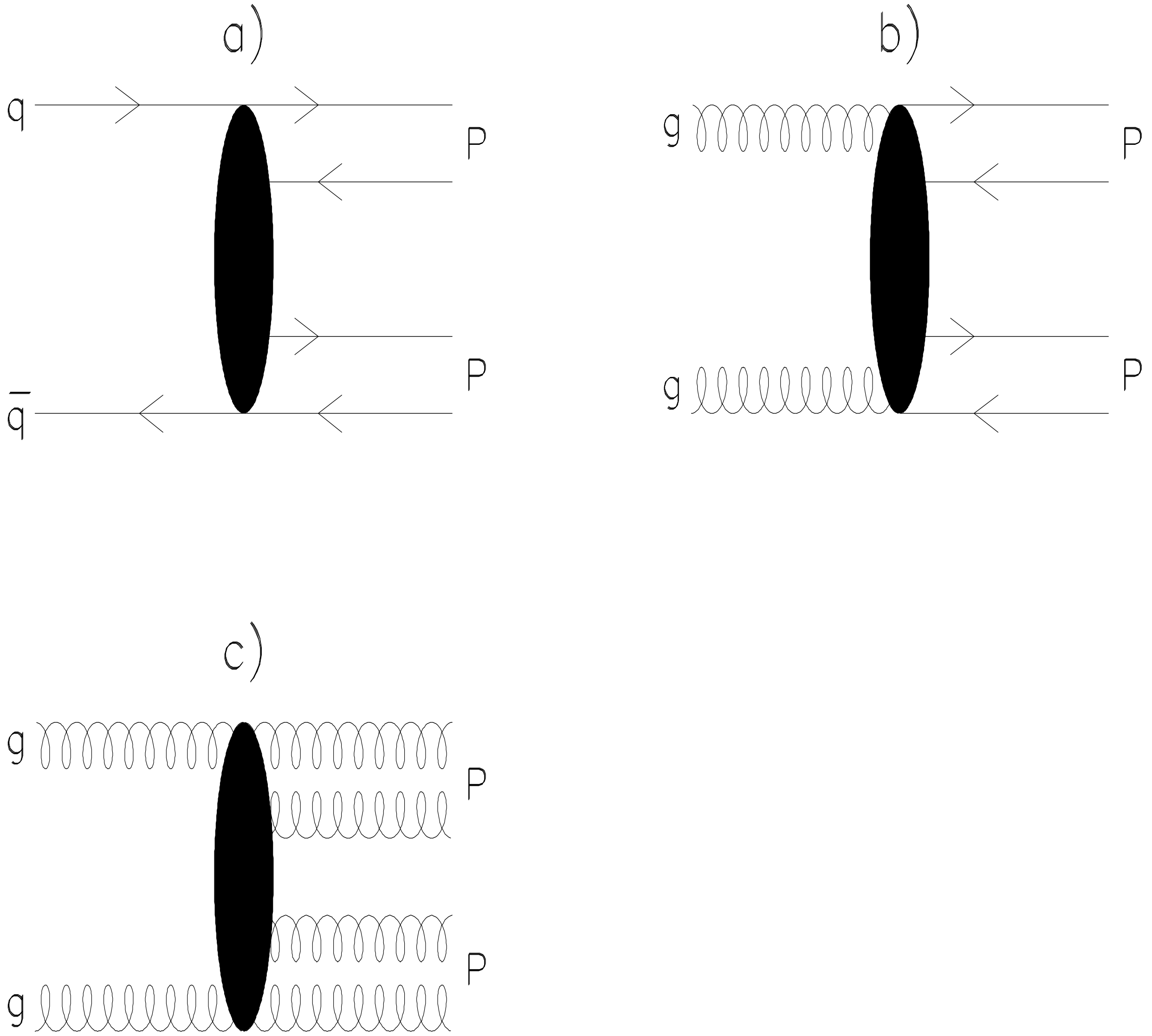

Figure 1

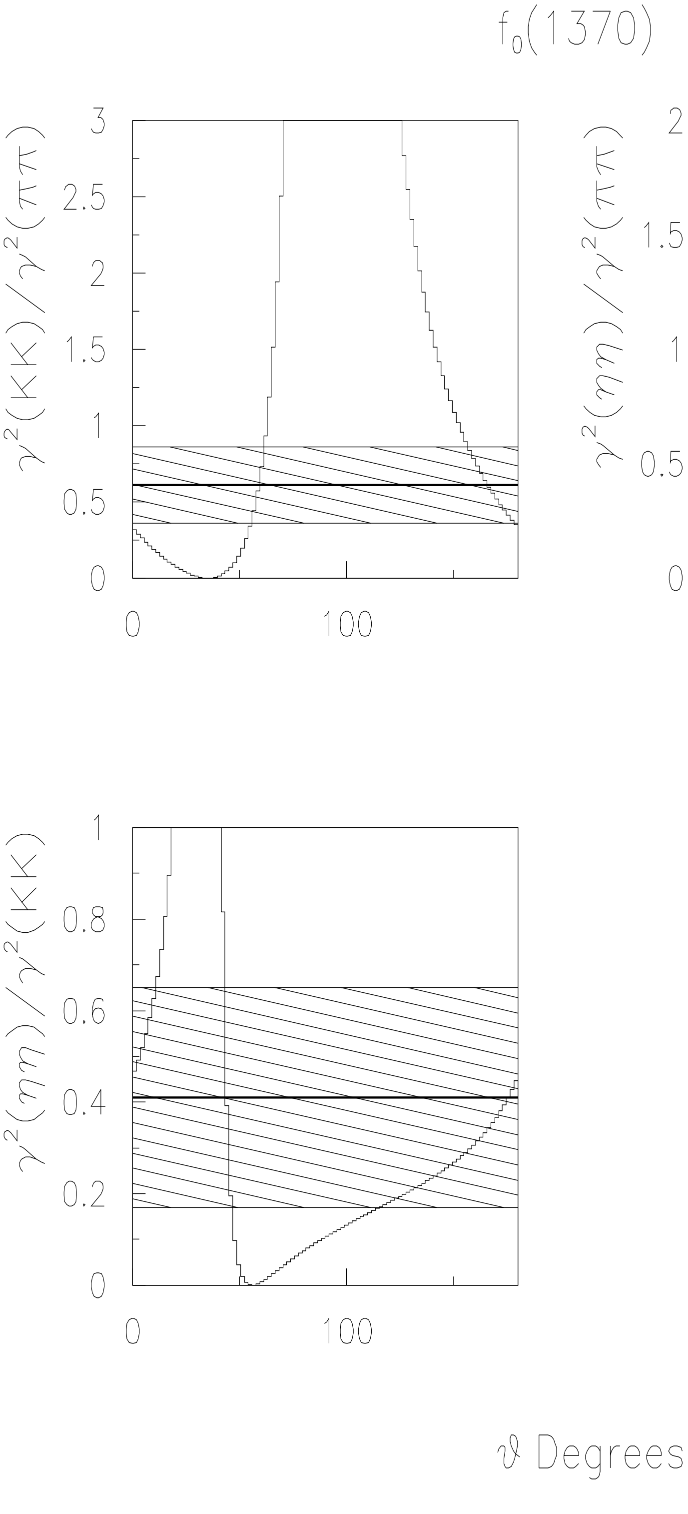

$f_0(1370)$
$\gamma^2(KK)/\gamma^2(\pi\pi)$
$\gamma^2(\eta\eta)/\gamma^2(\pi\pi)$
$\gamma^2(\eta\eta)/\gamma^2(KK)$
0
0.5
1
1.5
2
2.5
3
0.2
0.4
0.6
0.8
100
ϑ Degrees

Figure 2

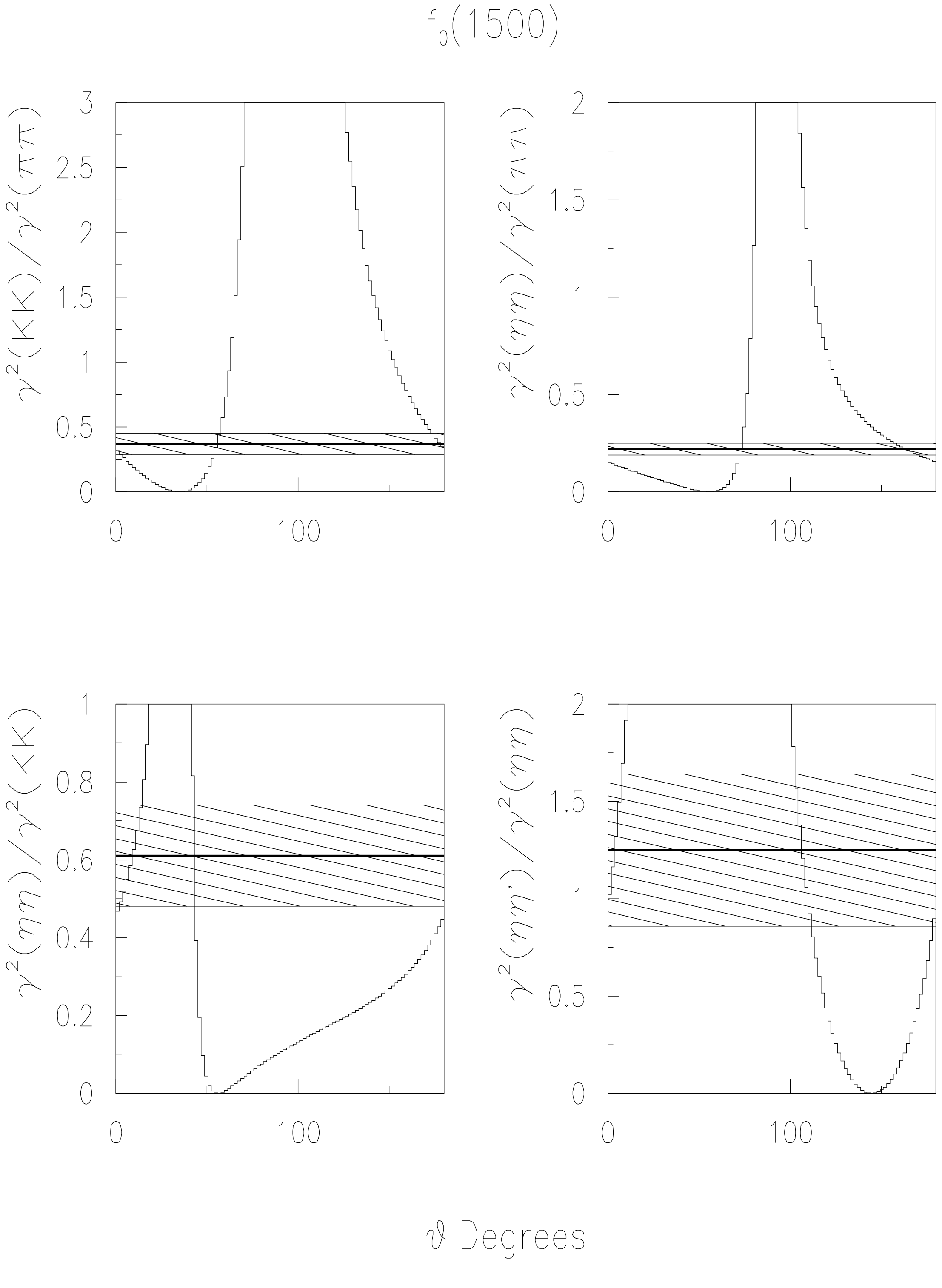
$f_0(1500)$
$\gamma^2(KK)/\gamma^2(\pi\pi)$
$\gamma^2(\eta\eta)/\gamma^2(\pi\pi)$
$\gamma^2(\eta\eta)/\gamma^2(KK)$
$\gamma^2(\eta\eta')/\gamma^2(\eta\eta)$
0
100
ϑ Degrees

Figure 3

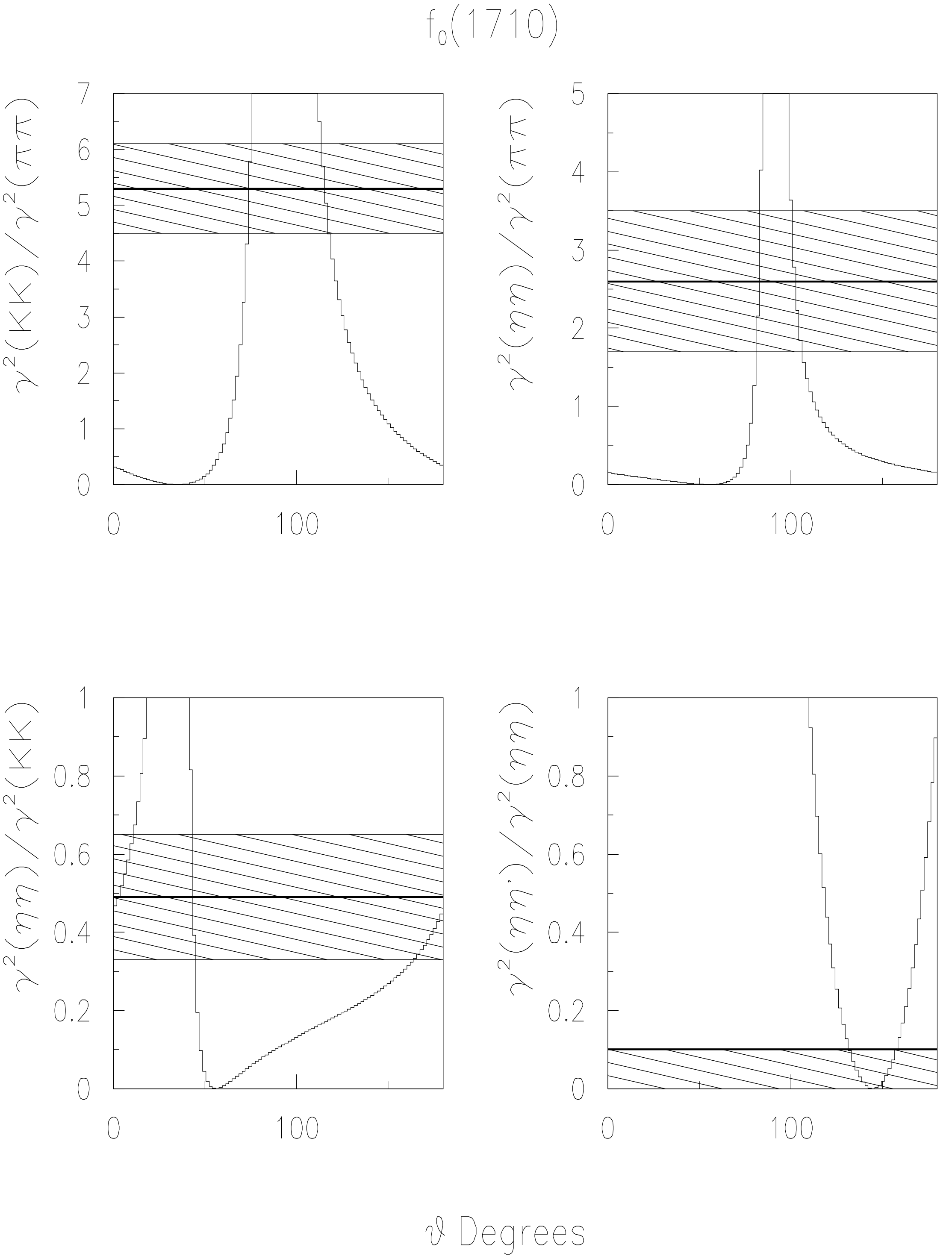

f0(1710)
γ²(KK)/γ²(ππ)
γ²(ηη)/γ²(ππ)
γ²(ηη)/γ²(KK)
γ²(ηη')/γ²(ηη)
0
100
ϑ Degrees

Figure 4